MECHANICAL BEHAVIOR OF I-BEAMS REINFORCED BY UNIDIRECTIONAL CARBON FIBRE, UNIDIRECTIONAL GLASS FIBRE AND CARBON FIBRE LAMINATES

Ilgar Jafarli, Umesh-Haribhai Vavaliya
Riga Technical University, Latvia
ilgar.jafarli@edu.rtu.lv, umesh-haribhai.vavaliya@rtu.lv

Abstract. Industry demands new engineering and material solutions. One of these solutions are fibre reinforced polymers. They are light and strong for application as a material for I-beams. An I-beam is the best section for a homogeneous material because of the highest resistance moment. The popularity of composite materials introduces wide use in most branches of engineering and mostly as fibre reinforced polymers (FRP). This paper presents numerical and analytical studies on the mechanical behaviour of the I-beams made of fibre reinforced polymers reinforced by glass fibres (GFRP) and carbon fibres (CFRP) comparing to the structural steel S235JR. Five I-beams with different composite structures and one steel I-beam were numerically tested. Four-point test according to ASTM C 78 – 02 was conducted. Numerical simulation made in SOLIDWORKS software in the Static simulation mode was used. The obtained results were analysed and an attempt to determine the optimal parameters for combination of different composite materials was conducted. As a result of numerical analysis values of deflection and normal stress were obtained for polymer I-beam reinforced by glass and carbon fibres comparing to the steel I-beam.

Keywords: carbon fibre, fibre reinforced polymer, glass fibre, I-beam, finite element method.

Introduction

Fibre reinforced polymer (FRP) composite beams are becoming very popular and used often in different engineering areas. Comparing to the mostly used traditional materials such as steel or wood, fibre reinforced polymer beams are more corrosion resistant, have advantageous weight-to-stiffness and weight-to-strength ratio and could be adjusted for exact application what makes them very flexible in terms of application [1-5].

Fibre reinforced polymer composite beams are already successfully used in fields like automotive, civil, naval and etc. engineering [6]. Mainly composite beams are designed depending on a specific task, what is exactly their purpose. For example, the FRP pedestrian bridge built in Okinawa or Tainan is made of specific continuous girders [7-9]. It is difficult to unify cross-section parameters, composite material parameters and thus makes it difficult to replace already existing steel structural I-beams. GFRP and CFRP beams are lighter than steel beams. Though GFRP is much cheaper than CFRP, it has smaller stiffness than CFRP and steel [7; 10]. Therefore, there are difficulties in usage of GFRP materials for heavy duty bridges and constructions due to the deflections. One of the ways to overcome this problem, is to use additional reinforcement in glass fibre reinforced polymer, to use carbon fibre reinforced polymer instead of glass carbon reinforced polymer. It can help architects make better constructions and give more freedom in shaping.

Novelty of this work is an attempt to find an optimal combination material and its parameters using the numerical study finite element method for the shape of a standard I-beam cross-section which is the best section for a homogeneous material because of the highest resistance moment.
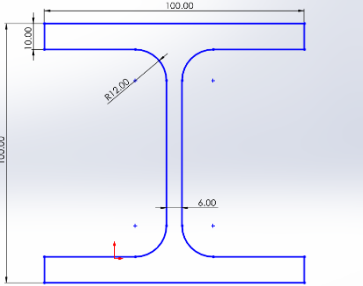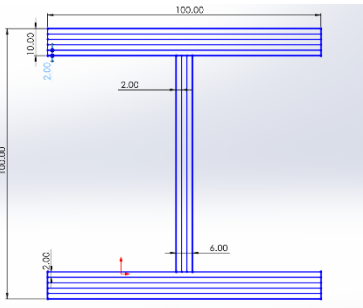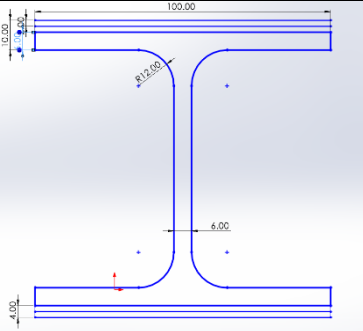
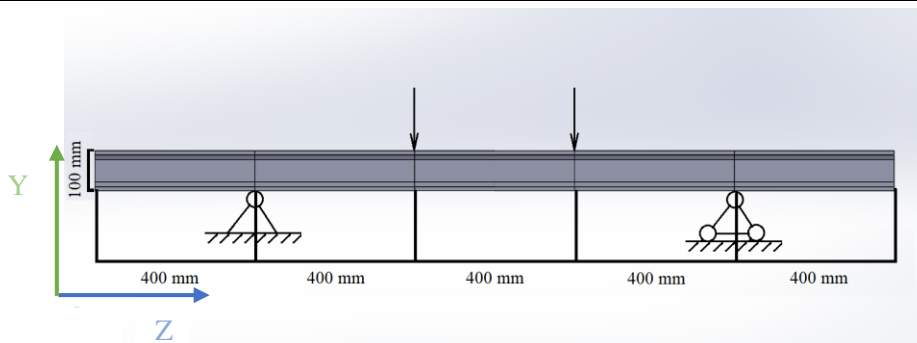## Materials and methods of the simulation

The experiment results were obtained by the finite element method using computer simulation on SOLIDWORKS software. The I-beam with cross-section HE100B by Euronorm 53-62 standard was used [11;12].

The cross-section size characteristics are shown below in Table 1. For the fully laminated composite I-beam was used a model made from laminates with difference in fillet radius. For the laminated I-beam the fillet radius is zero. The I-beam was tested by static simulation mode. Comparison of the results of the four-point test was made. Four-point test was conducted according to the ASTM C 78 – 02 standard [13]. The setup scheme for the four-point test is shown in Figure 1.

Table 1

Materials and beams

Number of beam	Type of beam	Cross-section	Material
1	S235JR		S235JR Structural steel
2	GF40%		40% reinforced GRFP Unidirectional
3	CF40%		40% reinforced CRFP Unidirectional
4	CFLW40% Unidirectional laminas		40% reinforced CRFP Laminated by woven [0º/90º/0º/90º/0º] flanges and [0º/90º/0º] web. Each ply is 2 mm
5	CFLW40% Bidirectional laminas		40% reinforced CRFP Laminated by woven [0º/90º/-45º/45º/0º/90º/45º/-45º/90º/0º] flanges and [0º/45º/90º/90º/45º/0º] web. Each ply is 2 mm and woven
6	CF40% + CFLW Bidirectional laminas		40% reinforced CRFP Unidirectional Laminated by woven reinforcement [0º/90º/90º/0º] flanges and unidirectional web. Each ply is 2 mm and woven

Fig. 1. **Setup scheme for the four-point test (ASTM C 78 – 02)**

As it was described above, six different materials and different configurations of them were used for the testing. The test was done using the finite element method on Solidworks simulation software static simulation mode [14-16]. The left cr¯oss-section of the beam translationally fixed and free in rotation. The right part translationally fixed only in *X* axis and *Y* axis directions and free in rotation,

while in Z axis direction it is free to move. Two forces applied each 10 000 N. Total length of the testing beam is 2000 mm.
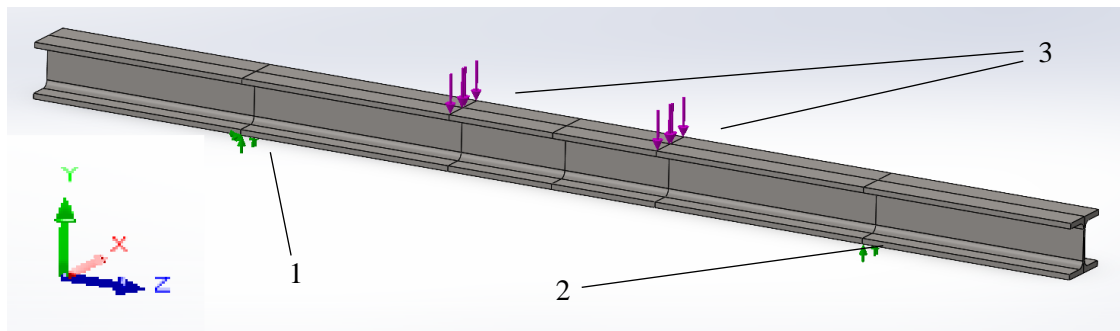

Fig. 2. **SOLIDWORKS setup:** 1 – fixed edge in *X*, *Y*, *Z* directions;
2 – fixed edge in *X*, *Y* directions; 3 – applied forces each 10 000 N

The setup scheme is shown in Figures 1 and 2. At the cross-section 1 in Figure 2 the lower edge of the lower flange is translationally fixed in *X*, *Y* and *Z* directions but free in rotation. At the cross-section 2 in Figure 2 the lower edge of the lower flange is translationally fixed only in *X* and *Y* directions and free in rotation. At the cross-section 3 in Figure 2 two forces are applied each 10 000 N on the upper edge of the upper flange.

Six different materials and different configurations of them for the same geometry cross-section I-beams were tested. The properties of materials are given in references [17-22]. Knowing the mechanical properties of each constituent material of the composite material, it is possible to find the properties of the 40% reinforced composite material properties using the rule of mixture (1) and Halpin-Tsai (2) equations [23; 24]. In this case, the woven composite material will be modelled as a 2-layer unidirectional composite material. The rule of mixtures (1) will be used to find the Young's modulus along the reinforcement direction.

$$E_{c1} = F_{f1} \cdot V_f + E_{m1} \cdot V_m , \qquad (1)$$

where E_{c1} – Young's modulus longitudinally of composite, Pa;
　　　　E_{f1} – Young's modulus longitudinally of fibre, Pa;
　　　　V_f – volume fraction of the fibre, m³;
　　　　V_m – volume fraction of the matrix, m³.

To calculate in the transverse direction, Halpin-Tsai equations are used.

$$E_{c2} = E_{m1} \cdot \frac{1 + \xi_1 \cdot \eta_1 \cdot V_f}{1 - \eta_1 \cdot V_f} , \qquad (2)$$

where E_{c2} – Young's modulus transversally of composite, Pa;
　　　　E_{m1} – Young's modulus longitudinally of matrix ($E_{m1} = E_{m2}$), Pa;
　　　　η_1 – Halpin-Tsai coefficient, Unitless.
　　　　ξ_1 – Halpin-Tsai coefficient (at $\xi_1 = 2$ gives accurate E_{c2} values), Unitless.

η_1 from equation (2) and η_2 is found by formulas (3) and (4).

$$\eta_1 = \frac{E_{f1} - E_{m1}}{E_{f1} + \xi_1 \cdot E_{m1}} , \qquad (3)$$

$$\eta_2 = \frac{G_{f12} - G_{m12}}{G_{f12} + \xi_2 \cdot G_{m12}} , \qquad (4)$$

where η_2 – Halpin-Tsai coefficient, Unitless;
　　　　ξ_2 – Halpin-Tsai coefficient (at $\xi_2 = 1$ gives accurate E_{c2} values), Unitless;
　　　　G_{f12} – Shear modulus longitudinally of fibre, Pa;
　　　　G_{m12} – Shear modulus of matrix longitudinally ($G_{m12} = G_{m23}$), Pa.

Shear modulus and Poison's ratios are found by formulas (5) and (6).

$$G_{c12} = G_{m12} \cdot \frac{1 + \xi_2 \cdot \eta_1 \cdot V_f}{1 - \eta_1 \cdot V_f}, \qquad (5)$$

where G_{c12} – shear modulus longitudinally of composite ($G_{c12} = G_{c23}$), Pa.

Shear modulus and Poison's ratios are found by formulas (5) and (6).

$$v_{c21} = \frac{E_{c2}}{E_{c1}} \cdot v_{c12}, \qquad (6)$$

where v_{c21} – Poison's ratio transversally of composite, Unitless;
v_{c12} – Poison's ratio longitudinally of composite, Unitless.

After finding these values, it is possible to start simulation of the materials. For the glass fibre composite, the same steps were applied. The obtained results are shown in Table 1.

Table 1

Mechanical properties of the obtained composites

Mechanical properties		Units	40% reinforced CRFP	40% reinforced GRFP
Young's modulus	E11	GPa	94.4	37.2
	E22		11.35	37.2
Shear modulus	G12	GPa	29.27	2.4
	G23		29.27	2.4
Poison's ration	v12	–	0.29	0.29
	v23		0.035	0.29
Density		kg·m^{-3}	1478	1786

Results and discussion

In this test 6 variants of HE100B and its composite analogues were tested. The I-beam was simulated using a curvature-based mesh with 10.67 mm largest element size and 3.55 mm smallest element size configuration. Maximal values of the normal stress at the stress force applying points are neglected and filtered from the results by Saint-Venant's principle [25]. The deflection along Y axis is denoted as u_y and the normal stress along Z axis is denoted as σ_z. The main interest is focused on the deflection rate u_y.

Table 2

Results

Beam number	I-beam	uy_{max}, mm	σz_{max}, N·m^{-2}
1	S235JR	-1.47E + 00	8.91E + 07
2	GF40%	-8.36E + 00	8.91E + 07
3	CF40%	-3.46E + 00	8.98E + 07
4	CFLW40% Unidirectional laminas	-5.29E + 00	1.17E + 08
5	CFLW40% Bidirectional laminas	-5.94E + 00	1.36E + 08
6	CF40% + CFLW Bidirectional laminas	-4.10E + 00	1.00E + 08

The beam number 1 is the etalon beam. Deflection rate of the beam which is closer to the deflection rate of the beam number 1 is counted as the optimal option. All of the FRP beams are lighter than the steel beam. According to the results obtained by the finite element method the closest to the I-beam number 1 in terms of the deflection is the I-beam number 3. But still there is a large difference comparing to the steel I-beam (number 1), 1.47 mm for the beam number 1 and 3.46 mm for the beam number 3. Perhaps, the deflection rate could be decreased by increasing the reinforcement ratio from 40% to 60% and more. Glass fibre I-beam (number 2) has the largest deflection rate. The normal stresses shown are the normal stresses at the top flange of the I-beam. According to the materials properties [14-19] the normal stresses are acceptable. It opens new opportunities for future tests and experiments of new configurations of the reinforcement materials especially in the I-beam cross-section shape. So,

considering the mass difference, the obtained results could be used for finding optimal solutions depending on the purpose of the I-beam.
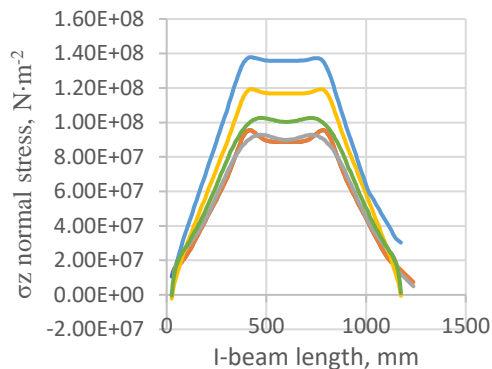

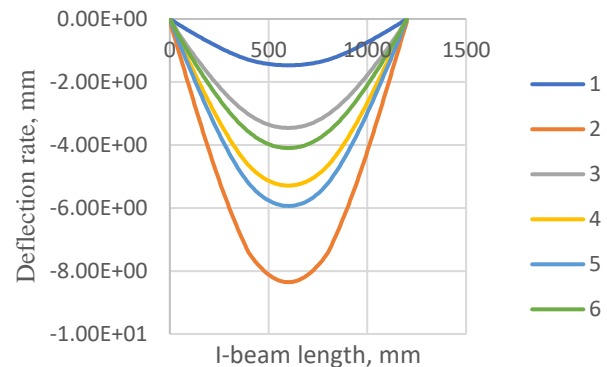Fig. 3. **Normal stress in Z axis**   Fig. 4. **Deflection in Y axis**

Conclusions

According to the results obtained by the finite element method the analysis showed results in favour of the unidirectional reinforcement rather than layered reinforcement. Carbon fibre I-beams are closer to steel by the elastic properties but much lighter. One cubic meter of 40% carbon fibre reinforced polymer weights 1478 kg (found using the rule of mixture) but 1 cubic meter of steel weights 7800 kg. Almost 5.28 times 40% reinforced carbon fibre is lighter than steel. This opens new opportunities for I-beams to be used for different architectural application due to the weight. Perhaps, carbon fibre I-beams with larger reinforcement ratio could show the desired mechanical behaviour with less deflection. For further and more detailed analysis experiments should be conducted. Glass fibre I-beams could be used for less loaded application rather than carbon fibre I-beams. Carbon fibre I-beams can be an alternative for steel I-beams.

Author contributions

Writing, editing, simulation and conceptualization I. Jafarli; CAD modelling and software consulting U.H. Vavaliya. All authors have read and agreed to the published version of the manuscript.

References

[1] Keller T., Rothe J., De Castro J., Osei-Antwi M., Asce S. M. GFRP-Balsa Sandwich Bridge Deck: Concept, Design, and Experimental Validation, 2013. DOI: 10.1061/(ASCE)CC.1943-5614.0000423
[2] Goh G. D., Dikshit V., Nagalingam A. P., Goh G. L., Agarwala S., Sing S. L., Wei J., Yeong W. Y. Characterization of mechanical properties and fracture mode of additively manufactured carbon fiber and glass fiber reinforced thermoplastics. Materials and Design, 137, 2018, pp. 79-89. DOI: 10.1016/j.matdes.2017.10.021
[3] Li Y. F., Badjie S., Chiu Y. T., Chen W. W. Placing an FRP bridge in Taijiang national park and in virtual reality. Case Studies in Construction Materials, 8, 2018, pp. 226-237. DOI: 10.1016/j.cscm.2018.02.005
[4] Wojcieh L., Maciej.K. Introduction to hybrid sections and hybrid beams in bridges. [online] [30.04.2022]. Available at: https://www.researchgate.net/publication/357689216
[5] Keller T., Haas C., Vallée T. Structural Concept, Design, and Experimental Verification of a Glass Fiber-Reinforced Polymer Sandwich Roof Structure. DOI: 10.1061/ASCE1090-0268200812:4454
[6] Tsai S.W., Hahn H.T. Introduction to composite materials. Routledge, 2018.
[7] Hai N. D., Mutsuyoshi H., Asamoto S., Matsui T. Structural behavior of hybrid FRP composite I-beam. Construction and Building Materials, 24(6), 2010, pp. 956-969. DOI: 10.1016/j.conbuildmat.2009.11.022
[8] Ueda T., Tamon U. FRP for construction in Japan Large rupture strain (LRS) fiber-reinforced polymer (FRP) composites for construction View project Performance prediction of structures with

damages View project FRP for construction in Japan. [online] [30.04.2022]. Available at: https://www.researchgate.net/publication/237784282

[9] Li Y. F., Badjie S., Chen W. W., Chiu Y. T. Case study of first all-GFRP pedestrian bridge in Taiwan. Case Studies in Construction Materials, 1, 2014, pp. 83-95. DOI: 10.1016/j.cscm.2014.05.001

[10] Goh G. D., Dikshit V., Nagalingam A. P., Goh G. L., Agarwala S., Sing S. L., Wei J., Yeong W. Y. Characterization of mechanical properties and fracture mode of additively manufactured carbon fiber and glass fiber reinforced thermoplastics. Materials and Design, 137, 2018, pp. 79-89. DOI: 10.1016/j.matdes.2017.10.021

[11] Warmgewalzte breite I-Träger (I- Breirflanschträger) mit parallelen Flanschflächen. [online] [24.11.2022]. Available at: https://op.europa.eu/en/publication-detail/-/publication/b05be6cb-cf92-47a2-8a33-ff874bd09e9d S1359835X05000357 (In German)

[12] Steel beams according to EN-10025/S355J2. [online] [24.11.2022]. Available at: https://www.stad.fr/en/steel-beams-columns-stock-profile-he-100-b.html

[13] Standard Test Method for Flexural Strength of Concrete (Using Simple Beam with Third-Point Loading). [online] [24.11.2022]. Available at: https://normanray.files.wordpress.com/2010/10/kuliah-7-c78.pdf

[14] Kononova O., Jevstignejevs V., Pupurs A., Kulkarnia A. Modelling micro-damage development in functionally graded knitted and woven carbon/steel fibre composites. Proceedings of the 20th European Conference on Composite Materials, June 26-30, 2022, Lausanne, Switzerland, pp. 298-305.

[15] Lusis V., Annamaneni K.K., Kononova O., Korjakins A., Lasenko I., Karunamoorthy R.K., Krasnikovs A. Experimental Study and Modelling on the Structural Response of Fiber Reinforced Concrete Beams (2022) Applied Sciences (Switzerland), 12 (19), art. no. 9492

[16] Lusis V., Kononova O., Macanovskis A., Stonys R., Lasenko I., Krasnikovs A. Experimental investigation and modelling of the layered concrete with different concentration of short fibers in the layers (2021) Fibers, 9 (12), art. no. 76

[17] Kumar N.S., Kumar G.V., Kumar C.V., Prabhu M. Experimental Investigation on Mechanical Behavior of E-Glass and S-Glass Fiber Reinforced with Polyester Resin. SSRG International Journal of Mechanical Engineering, vol. 5, no. 5, 2018, pp. 19-26. DOI: 10.14445/23488360/IJME-V5I5P104

[18] Mild steel S235JR VS S235J2 steel. [online] [24.11.2022]. Available at: http://www.bbnsteelplate.com/news·m^{-1}ild-steel-s235jr-vs-s235j2-steel_948.html

[19] Wang W., Dai Y., Zhang C., Gao X., Zhao M. Micromechanical Modeling of Fiber-Reinforced Composites with Statistically Equivalent Random Fiber Distribution. Materials, 9(8), 2016. DOI: 10.3390·m^{-1}a9080624

[20] Hexcel® HexPly® 914 175°C Curing Epoxy Matrix. [online] [24.11.2022]. Available at: https://www.matweb.com/search/datasheettext.aspx?matguid = 10199622b9ba408c83347d0dc63bf686

[21] T300 standard modulus carbon fiber. [online] [24.11.2022]. Available at: https://www.toraycma.com/wp-content/uploads/T300-Technical-Data-Sheet-1.pdf.pdf

[22] Ovako S235JR EN10025-2 (ref) Steel, + AR. [online] [24.11.2022]. Available at: https://www.matweb.com/search/datasheet.aspx?matguid = ffc482278e2e4dc780572160dcada3d1

[23] Halpin J. C., Louis S. T., Kardos J. L. The Halpin-Tsai Equations: A Review. [online] [24.11.2022]. Available at: https://www.uio.no/studier/emner·m^{-1}atnat·m^{-1}ath/nedlagte-emner·m^{-1}EK4540/h09/undervisningsmateriale/halpintsai_review.pdf

[24] Halpin J.C. Primer on Composite Materials Analysis. Second Edition, Revised. Taylor and Francis Group, 1992. 240 p.

[25] Тимошенко С. П., Гудьер Дж. Теория упругости (Theory of elasticity). М.: Наука, 1979. 560 p. (In Russian).